学位論文

β_3-Adrenergic receptor blockade reduces mortality in endotoxin-induced heart failure by suppressing induced nitric oxide synthase and saving cardiac metabolism

（β_3アドレナリン受容体遮断は、エンドトキシン起因の敗血症性心不全における誘導型一酸化窒素合成酵素を抑制し、心筋代謝を改善する事で生存率を改善する）

旭川医科大学大学院医学系研究科博士課程医学専攻

川口　哲

（岡田基、井尻えり子、甲賀大輔、渡部剛、林健太郎、柏木友太、藤田智、長谷部直幸と共著）

Am J Physiol Heart Circ Physiol 318: H283–H294, 2020.
First published December 13, 2019; doi:10.1152/ajpheart.00108.2019.

RESEARCH ARTICLE | *Integrative Cardiovascular Physiology and Pathophysiology*

β_3-Adrenergic receptor blockade reduces mortality in endotoxin-induced heart failure by suppressing induced nitric oxide synthase and saving cardiac metabolism

Satoshi Kawaguchi,[1] Motoi Okada,[1] Eriko Ijiri,[1] Daisuke Koga,[2] Tsuyoshi Watanabe,[2] Kentaro Hayashi,[3] Yuta Kashiwagi,[3] Satoshi Fujita,[1] and Naoyuki Hasebe[4]

[1]Department of Emergency Medicine, Asahikawa Medical University, Asahikawa, Hokkaido, Japan; [2]Department of Microscopic Anatomy and Cell Biology, Asahikawa Medical University, Asahikawa, Hokkaido, Japan; [3]Department of Anesthesiology and Critical Care Medicine, Asahikawa Medical University, Asahikawa, Hokkaido, Japan; and [4]Respiratory and Neurology Division, Department of Internal Medicine, Cardiovascular, Asahikawa Medical University, Asahikawa, Hokkaido, Japan

Submitted 29 March 2019; accepted in final form 4 December 2019

Kawaguchi S, Okada M, Ijiri E, Koga D, Watanabe T, Hayashi K, Kashiwagi Y, Fujita S, Hasebe N. β_3-Adrenergic receptor blockade reduces mortality in endotoxin-induced heart failure by suppressing induced nitric oxide synthase and saving cardiac metabolism. *Am J Physiol Heart Circ Physiol* 318: H283–H294, 2020. First published December 13, 2019; doi:10.1152/ajpheart.00108.2019.—The β_3-adrenergic receptor (β_3AR) is related to myocardial fatty acid metabolism and its expression has been implicated in heart failure. In this study, we investigated the role of β_3AR in sepsis-related myocardial dysfunction using lipopolysaccharide (LPS)-induced endotoxemia as a model of cardiac dysfunction. We placed mice into three treatment groups and treated each with intraperitoneal injections of the β_3AR agonist CL316243 (CL group), the β_3AR antagonist SR59230A (SR group), or normal saline (NS group). Survival rates were significantly improved in the SR group compared with the other treatment groups. Echocardiography analyses revealed cardiac dysfunction within 6–12 h of LPS injections, but the outcome was significantly better for the SR group. Myocardial ATP was preserved in the SR group but was decreased in the CL-treated mice. Additionally, quantitative PCR analysis revealed that expression levels of genes associated with fatty acid oxidation and glucose metabolism were significantly higher in the SR group. Furthermore, the expression levels of mitochondrial membrane protein complexes were preserved in the SR group. Electron microscope studies showed significant accumulation of lipid droplets in the CL group. Moreover, inducible nitric oxide synthase (iNOS) protein expression and nitric oxide were significantly reduced in the SR group. The in vitro study demonstrated that β_3AR has an independent iNOS pathway that does not go through the nuclear factor-κB pathway. These results suggest that blockading β_3AR improves impaired energy metabolism in myocardial tissues by suppressing iNOS expression and recovers cardiac function in animals with endotoxin-induced heart failure.

NEW & NOTEWORTHY Nitric oxide production through stimulation of β_3-adrenergic receptor (β_3AR) may improve cardiac function in cases of chronic heart failure. We demonstrated that the blockade of β_3AR improved mortality and cardiac function in endotoxin-induced heart failure. We also determined that LPS-induced inducible nitric oxide synthase has a pathway that is independent of nuclear factor-κB, which worsened cardiac metabolism and mortality in the acute phase of sepsis. Treatment with the β_3AR antagonist had a favorable effect. Thus, the blockade of β_3AR could offer a novel treatment for sepsis-related heart failure.

β_3-adrenergic receptor; cardiac metabolism; endotoxin-induced heart failure; lipopolysaccharide; sepsis

INTRODUCTION

Sepsis is a systemic inflammatory response to bacterial infection. Cardiac dysfunction is a critical consequence of sepsis, with mortality reflecting either elevated levels of inflammation or suppression of fatty acid and glucose oxidation and eventual depletion of adenosine triphosphate (ATP) (1). Reportedly, β-adrenergic signaling is compromised in animal models and patients with sepsis, further aggravating heart dysfunction (8, 9, 27). Heart tissues produce ATP primarily through fatty acid and glucose oxidation, both of which decline markedly in experimental animal models of sepsis (10, 11). Thus, the impacts of this disease on metabolic pathways and in adrenergic signaling, along with the potential interplay of the latter with inflammation, remain unclear.

Recent studies have indicated that the numbers of β_3-adrenergic receptors (β_3AR) increase in chronically failing hearts and that stimulation of β_3AR can protect against heart failure by regulating myocardial nitric oxide (NO) synthase and modulating oxidative stress (2, 16, 18, 23). However, little is known about the role of β_3AR in failing heart tissues during the onset of sepsis. Activation of β_3AR might exacerbate septic cardiac damage because of the negative cardiac inotropic effects of inducible nitric oxide synthase (iNOS)-induced NO generation and excessive lipolysis, which leads to cardiac lipotoxicity.

Endotoxins have been shown to mediate cardiovascular changes that mimic sepsis in research animals and human volunteers (26). Stimulation of β-adrenergic activity during sepsis is blunted by alterations at various levels in this signaling cascade. Accordingly, in patients with reduced left ventricular function and septic mice, decreased β-adrenergic responses are associated with elevated levels of NO (14, 26).

Address for reprint requests and other correspondence: M. Okada, Dept. of Emergency Medicine, Asahikawa Medical Univ., 2-1-1-1 Midorigaoka-Higashi, Asahikawa, Hokkaido 078-8510, Japan (e-mail: motoy@asahikawa-med.ac.jp).

Lipopolysaccharide (LPS) has systemic effects that result in a sepsis-like condition that is characterized by hypotension and widespread tissue damage, including myocardial dysfunction. In this study, we hypothesized that β_3AR regulates fatty acid oxidation in failing heart tissues and investigated its roles following pharmacological interventions with β_3AR agonists and antagonists in an LPS-induced model of cardiac dysfunction.

MATERIALS AND METHODS

This study was conducted with the approval of the Institutional Review Board of Asahikawa Medical University. All procedures involving animals were conducted in accordance with the National Institutes of Health Guide for the Care and Use of Laboratory Animals and were approved by the Institutional Animal Care and Use Committee of Asahikawa Medical University.

Experimental animals. Male C57Bl/6 mice (8–10 wk) weighing 22–25 g were purchased from Charles River Laboratories Japan (Yokohama, Japan) and were housed for at least 1 wk under a 12-h:12-h light-dark cycle at 21–23°C. Animals were fed a standard chow diet and were given water ad libitum before and during experiments.

Reagents. The specific β_3AR agonist CL316243 and the specific β_3AR antagonist SR59230A were purchased from Sigma-Aldrich (Tokyo, Japan). LPS (*Escherichia coli* O111) was purchased from FUJIFILM Wako Pure Chemical (Osaka, Japan).

Experimental protocol. Experimental sepsis was induced in male C57Bl/6 mice by administering intraperitoneal injections of LPS at 10 mg/kg. After 3 h, mice were allocated to three groups (n = 10 each) and were administered intraperitoneal CL316243 at 1 mg/kg (CL group), SR59230A at 1 mg/kg (SR group), or 200 μL of normal saline (NS group). A separate control group received intraperitoneal injections of saline only.

We evaluated cardiac function using echocardiography at 6, 12, and 24 h after LPS treatments. Thereafter, the mice in each group (n = 10) were euthanized using 2% isoflurane inhalation and hearts were harvested using thoracotomy at 12 h after LPS treatment. Excised hearts were flash frozen and stored at −80°C until analyses of myocardial ATP, investigations of gene and protein expression levels, and histopathological examinations.

Echocardiographic assessments. Cardiac function in septic mice was measured using a two-dimensional echocardiograph (Vevo2100 Primetech; Primetech, Tokyo, Japan) before and at 6, 12, and 24 h after LPS treatment. Echocardiographic assessments were performed by three observers who were blinded to the mice groups. Left ventricular fractional shortening (LVFS) and heart rate (HR) were measured in standard M mode, whereas left ventricular end-systolic volume (LVESV), left ventricular end-diastolic volume, and left ventricular ejection fraction (LVEF) were calculated using the single plane area-length method.

Measurements of blood parameters. Blood samples were taken from the vena cava upon euthanasia of mice, and serum levels of triacylglycerol and nonesterified fatty acid were determined using enzyme assays.

Analysis of myocardial ATP. ATP levels were determined in 30-mg myocardial tissue samples. To this end, tissues were dissolved and homogenized in 10 mM ice-cold HEPES-NaOH at pH 7.4 and were centrifuged at 1,000 *g* for 10 min at 4°C. Supernatants were then resuspended in 10 mM HEPES-NaOH at pH 7.4 and portions of supernatants were taken to determine ATP contents using kits (TOYO B-Net, Tokyo, Japan) according to the manufacturer's instructions. ATP contents were determined based on the optical activity of luciferase with firefly luciferin substrate.

RNA purification and gene expression analysis. RNA samples were purified from heart tissues using RNeasy mini (Qiagen Japan, Kanagawa, Japan) kits, according to the manufacturer's instructions. Subsequently, cDNA was synthesized using SuperScript III First-Strand (Invitrogen Japan, Tokyo, Japan) and analyzed using quantitative polymerase chain reactions (PCR) with TaKaRa LA Taq (TaKaRa, Tokyo, Japan). Primers for PCR are listed in Supplemental Table S1 (https://doi.org/10.6084/m9.figshare.10298456.v5).

Protein purification and analysis. Isolated heart tissues were homogenized on ice for 2 h in radioimmunoprecipitation assay lysis buffer (Santa Cruz Biotechnology, Dallas, TX) containing the protease inhibitors leupeptin (5 μg/mL), aprotinin (2 μg/mL), and phenylmethylsulfonyl fluoride (PMSF; 1 mM). Lysates were centrifuged at 12,000 *g* for 20 min at 4°C. After the collecting supernatants and determining protein concentrations, aliquots containing 50 mg of protein were separated by electrophoresis on 4–12% Blot Bis-Tris Plus Gels (Invitrogen Japan) in a NuPAGE MOPS SDS Running Buffer system (Invitrogen Japan) and were sequentially transferred electrophoretically to nitrocellulose membranes. After blocking with Tris-buffered saline containing Tween-20 (TBST) and 5% milk (TBST, milk), membranes were immunoblotted overnight at 4°C with anti-endothelial nitric oxide synthase (eNOS) antibody (1:500, ab76198; Abcam, Cambridge, MA), anti-iNOS antibody (1:200, sc-7278; Santa Cruz Biotechnology), anti-β_1-adrenergic receptor (β_1AR) antibody (1:1,000, ab3442; Abcam), anti-β_2-adrenergic receptor (β_2AR) antibody (1:1,000, ab182136; Abcam), anti-β_3AR antibody (1:1,000, LS-C353880; Lifespan Bioscience, Seattle, WA), anti-β actin antibody (1:1,000, no. 4967, Cell Signaling Technology, Danvers, MA), anti-nuclear factor-κB (NF-κB) p65 antibody (1:1,000, ab16502; Abcam), or anti-total mitochondrial oxidative phosphorylation (OXPHOS) antibody (1:250, ab110413; Abcam). Thereafter, the membranes were incubated with appropriate secondary antibodies conjugated with horseradish peroxidase at room temperature for 60 min. Protein bands were visualized using an enhanced chemiluminescence system (Amersham Bioscience, Buchingham-shire, UK). Densitometric analyses of visualized bands were performed using Image Processing and Analysis in Java (ImageJ) software.

Measurement of NO concentrations in myocardium. Myocardial tissue samples (50 μg) were homogenized in 0.1 M phosphate buffer (PB; pH 7.4) and then centrifuged at 12,000 *g* for 20 min at 4°C. NO concentrations of the resulting tissue supernatants were determined using QuantiChrom Nitric Oxide Assay Kits (BioAssay Systems, Hayward, CA) according to the manufacturer's instructions.

Mitochondria isolation. Mitochondrial proteins were extracted using a mitochondrial isolation kit (ab110169; Abcam), according to the

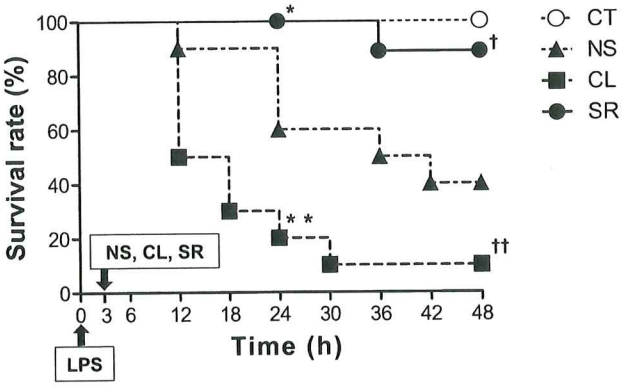

Fig. 1. Kaplan-Meier survival curves of mice with LPS-induced heart failure. Treatment with the β_3-adrenergic receptor (AR) antagonist SR59230A (SR) significantly reduced mortality, whereas treatment with the β_3AR agonist CL316243 (CL) exacerbated mortality. Kaplan-Meier survival curves of saline (NS)-treated mice (closed triangle), CL-treated mice (closed square), and SR-treated mice (closed circle); *P = 0.0172 vs. NS, **P = 0.0225 vs. NS, †P = 0.0181 vs. NS, ††P = 0.0190 vs. NS; n = 10 in each group. CT, control.

manufacturer's instructions. Heart tissues were washed and homogenized in ice-cold isolation buffer using a glass bounce homogenizer. Homogenates were then centrifuged at 1,000 *g* for 10 min at 4°C, and supernatants were transferred to fresh tubes and centrifuged again at 12,000 *g* for 15 min at 4°C. Cell pellets were then washed and resuspended as mitochondrial protein samples in 200-μL aliquots of isolation buffer. Samples were then immediately processed for protein analyses.

Histological analysis. Neutral and deposited lipids in septic hearts were assessed using oil red O staining. The hearts were embedded in an optimal cutting temperature compound (Tissue-Tek; Sakura Finetek Japan, Tokyo, Japan). Midportions of cardiac ventricles were cut into 5-μm slices and then stained with oil red O.

Scanning electron microscopy. At 12 h after LPS administration, mice were anesthetized and perfused with 10 mL of NS, followed by a mixture of 0.5% glutaraldehyde and 0.5% paraformaldehyde in 0.1 M PB (pH 7.4). Whole hearts were then removed from the mice, dissected into small pieces, and fixed with 1% osmium tetroxide (OsO_4) in 0.1 M PB for 2 h at 4°C. Thereafter, specimens were rinsed with 0.1 M PB for 1 h (10 min, 6 times) and immersed in 25 and 50% dimethyl sulfoxide (DMSO) in distilled water for 30 min each. Subsequently, the specimens were frozen on an aluminum block that had been precooled with liquid nitrogen and cracked into two pieces using a screwdriver and a hammer on a block. Fractured pieces were immediately placed in 50% DMSO to thaw at room temperature and rinsed in 0.1 M PB for 10 min (×6) until the DMSO was completely removed. To macerate cells, specimens were immersed in 0.1 M PB containing 0.1% OsO_4 for 96 h at 21°C. Macerated samples were then fixed in the same solution for 1 h. Subsequently, conductive staining was performed by treating the specimens with 0.1 M PB containing 1% tannic acid (Nacalai Tesque, Kyoto, Japan) for 1 h, washing in 0.1 M PB for 1 h, and immersing in 0.1 M PB containing 1% OsO_4 for 1 h. All specimens were dehydrated using a graded ethanol series, transferred to isoamyl acetate, and dried in a critical point dryer (HCP-2; Hitachi, Tokyo, Japan) with liquid CO_2. After checking fractured surfaces under a dissecting microscope, dried specimens were mounted on aluminum stubs with silver paste and lightly coated (<3 nm) with platinum and palladium in an ion-sputter coater (E1010; Hitachi). Finally, the specimens were observed under a field-emission scanning electron microscope (S-4100; Hitachi) at an accelerating voltage of 5 kV.

Immunohistochemistry. Mice hearts were embedded in an optimal cutting temperature compound (Tissue-Tek) and frozen in liquid nitrogen. The resulting blocks were cut into 5-μm sections. Sections were then permeabilized with 0.1% Triton X-100 in Tris-buffered saline for 10 min and blocked at room temperature for 30 min using 5% CAS-block. Sections were incubated overnight at 4°C with anti-mitochondrial cytochrome-*c* oxidase-1 (COX-1) antibody (Anti-MTCO1 antibody; Alexa Fluor 647, ab198600; Abcam) and were then washed with 0.1% TBST. Thereafter, cardiomyocytes were subjected to nuclear staining and immunofluorescence microscopy.

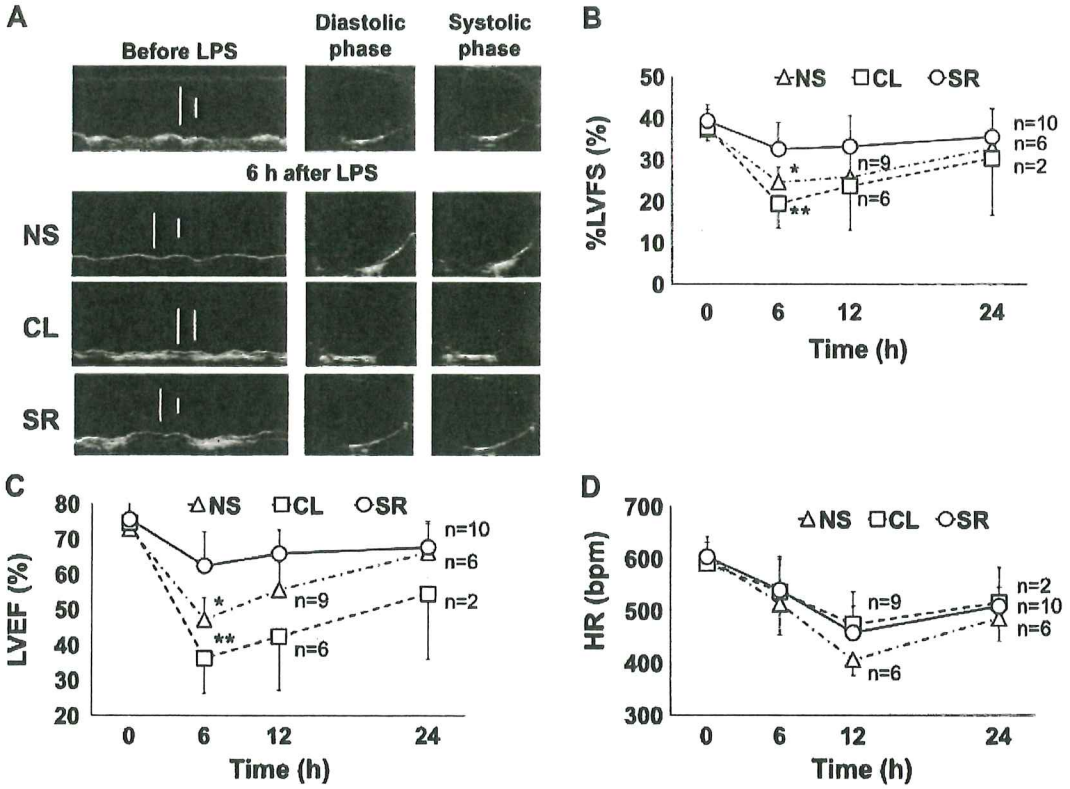

Fig. 2. Echocardiography evaluation of cardiac function. *A*: representative images (*left*: M mode; *right*: B mode) of the left ventricle in the long-axis view before and 6 h after lipopolysaccharide (LPS) injections; maximally reduced cardiac contractions were observed at 6 h after LPS administration in the normal saline (NS) and CL316243 (CL) groups, whereas cardiac contraction was preserved in the SR59230A (SR) group. *B* and *C*: these graphs indicate percentage left ventricular fractional shortening (%LVFS) and left ventricular ejection fraction (LVEF), respectively, which were measured from the long-axis M mode view at 6, 12, and 24 h after LPS administration. At 6 h, maximally decreased %LVFS and LVEF were observed in all groups, and these were recovered with time. The SR group did not show decreased %LVFS or LVEF. The CL group showed decreased %LVFS and LVEF compared with the NS group. *D*: heart rates (HR) at 6, 12, and 24 h after LPS administration. Maximally decreased HR were observed 12 h after LPS treatments and recovered thereafter, but no significant differences were observed between treatment groups; $*P < 0.05$ vs. SR, $**P < 0.05$ vs. SR; $n = 10$ in each group.

In vitro studies. In vitro experiments were performed using H9C2-cultured cardiomyoblasts as described in the Supplemental Materials and Supplemental Figs. S1 and S2.

Statistical analysis. Pairwise comparisons of mean values from three or more groups were performed using one-way analysis of variance, followed by Bonferroni post hoc tests. All values are presented as means ± SD. Survival rates were assessed using the Kaplan-Meier method and were compared between groups using the Mantel-Cox log-rank test. Differences were considered significant when $P < 0.05$.

RESULTS

Antagonism of β_3AR improved survival rates after LPS-induced cardiac failure. At 24 h after LPS treatments, mice of the SR group ($P = 0.0172$ vs. NS group) remained alive, whereas only 60% of mice in the NS group and 20% of mice in the CL group ($P = 0.0225$ vs. NS group) were alive. Furthermore, after 48 h, a 90% survival rate was observed in the SR group ($P = 0.0181$ vs. NS group), whereas that in the CL group was only 10% ($P = 0.0190$ vs. NS group). Kaplan-Meier analyses showed that mortality was significantly decreased by the β_3AR antagonist but significantly increased by the β_3AR agonist (Fig. 1).

β_3AR antagonist improved cardiac function. In the present experiments, cardiac dysfunction was apparent from 3 h after LPS injection. Moreover, diffuse hypokinesis and the lowest LVEF were observed at 6 h after LPS administration (Fig. 2*A*). Afterward, cardiac function was gradually restored and the damage was reversed. Notably, the SR group did not show decreased %LVFS or LVEF (%LVFS, 32.5 ± 6.4%; LVEF, 62.3 ± 9.7%; $P < 0.05$ vs. NS group, $n = 10$ in each group). In contrast, the CL group showed decreased LVEF with exacerbation of LVESV (%LVFS, 19.4 ± 5.9%; LVEF, 36.2 ± 10.0%; $P < 0.05$ vs. NS group, $n = 10$ in each group), when compared with the NS group (LVFS, 24.5 ± 3.6%; LVEF, 47.1 ± 6.2%; Fig. 2, *B* and *C*). In addition, survivors in the CL group needed much more time to recover cardiac function than survivors in the NS group. The HR also decreased at 12 h after LPS administration and recovered afterward (Fig. 2*D*). However, at 12 h, no significant differences in HR were observed between the three groups.

Upregulation of β_3AR expression in endotoxin-induced impaired hearts. Quantitative PCR and Western blot analyses of β-adrenergic receptor expression in LPS-damaged heart tissues showed that β_1AR expression decreased in all treatment groups (Fig. 3*A*) and β_2AR expression did not differ between the three LPS-treated groups and the saline-treated control group (Fig. 3*B*). In contrast, β_3AR expression was enhanced in all groups irrespective of the β_3AR-targeted agent (Fig. 3*C*).

β_3AR antagonist improved cardiac metabolism during endotoxin-induced heart failure. Myocardial ATP levels were significantly lower in the NS and CL groups than the saline-treated control group. However, myocardial ATP in the SR group was maintained at a higher level than in the NS and CL groups (1.25-fold and 1.54-fold, respectively; Fig. 4).

Regulation of myocardial iNOS by the β_3AR antagonist. Expression levels of iNOS mRNA and protein were markedly suppressed in the SR group but significantly elevated in the NS and CL groups (Fig. 5*A*). However, no significant differences in eNOS expression levels were noted between the groups (Fig. 5*B*), and LPS-induced NO production was reduced in the SR group (Fig. 5*C*). In agreement, our in vitro studies using H9C2 rat cardiomyoblast cells confirmed greater increases in iNOS following CL treatments than with LPS treatments alone. Knockdown of β_3AR by siRNA, however, significantly decreased iNOS expression (Supplemental Fig. S1B).

Other mediators of myocardial inflammation. The inflammatory transcription regulator NF-κB p65 was expressed at increased levels in myocardial tissues, but no significant ex-

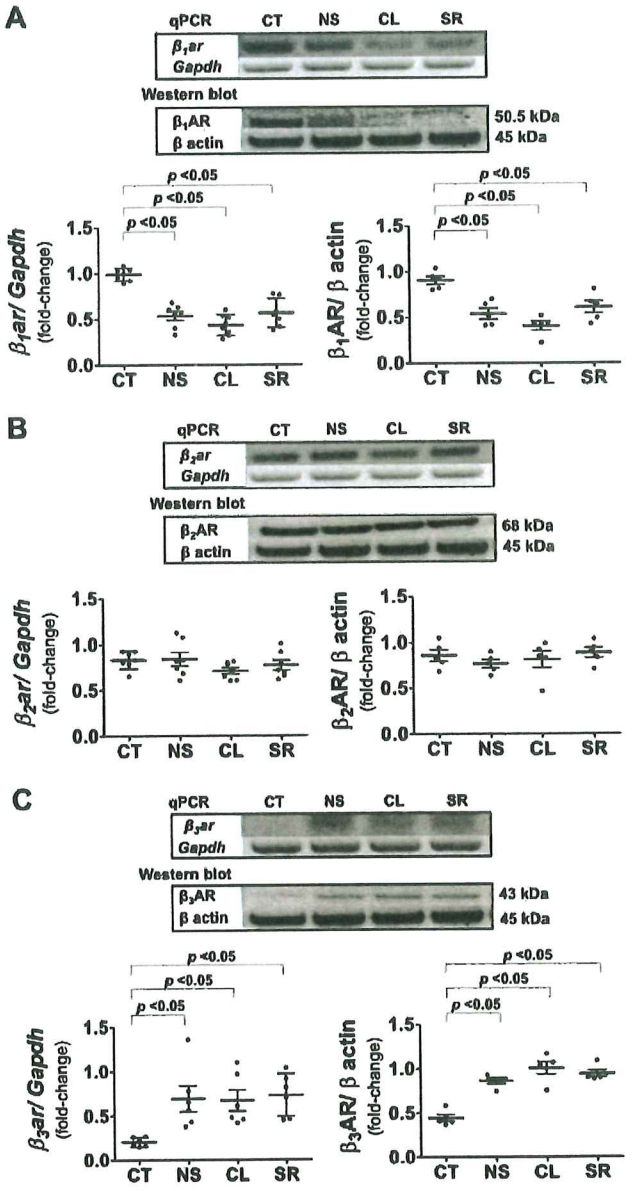

Fig. 3. β-Adrenergic receptor expression levels in the myocardium. *A*: quantitative polymerase chain reaction (PCR) and Western blot analyses show significant reductions in β_1-adrenergic receptor (AR) mRNA and protein expression following LPS treatments. No significant differences were observed between normal saline (NS), CL316243 (CL), and SR59230A (SR) groups. *B*: no significant differences in β_2AR mRNA and protein expression were observed. *C*: β_3AR mRNA and protein expression levels were increased by LPS but did not differ significantly between the NS, CL, and SR groups; n = 5–7 in each group. CT, control; qPCR, quantitative PCR.

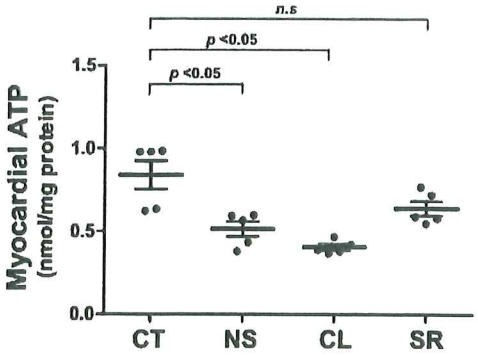

Fig. 4. Changes in myocardial ATP at 12 h after LPS administration. Myocardial ATP measurements were based on the optical activity of luciferase with the substrate firefly luciferin. Myocardial ATP concentrations were reduced in the normal saline (NS) and CL316243 (CL) groups but remained high in the SR59230A (SR) group. Values are presented as ATP per unit of absorbance in arbitrary units; n = 5. CT, control; n.s., not significant.

pression differences were found between the NS, CL, and SR groups (Fig. 6*A*). Downstream of NF-κB, the TNFα, IL6, and IL1β expression levels were increased in the NS, CL, and SR groups and did not differ between them (Fig. 6*B*).

Blockade of β_3AR improved myocardial fatty acid oxidation and glucose metabolism. To investigate the mechanisms through which myocardial ATP concentrations were preserved in the SR group, we determined the expression levels of proteins that are involved in fatty acid and glucose metabolism (Fig. 7*A*). Among these, the cluster of differentiation 36 (CD36) is a cellular importer of fatty acids, and its expression was unchanged in all treatment groups. In contrast, carnitine palmitoyltransferase 1 (CPT1), which transports fatty acids into mitochondria, was present at higher levels in the SR group than the CL and NS groups. Furthermore, the SR group showed significantly increased expression of peroxisome proliferator-activated receptor-γ coactivator 1α (PGC1α) and estrogen-related receptor-α (ERRα), which are implicated in mitochondrial biogenesis. Increased levels of peroxisome proliferator-activated receptor-α (PPARα), which is a regulator of fatty acid oxidation, were also observed in the SR group. In contrast, the expression of peroxisome proliferator-activated receptor-γ (PPARγ), which is involved in fatty acid oxidation and insulin resistance and has anti-inflammatory effects, was significantly decreased in the CL group but tended to increase in the NS group (Fig. 7*A*). We also investigated glucose oxidation, which produces ATP and is positively regulated by glucose transporter type 4 (GLUT4) and negatively regulated by pyruvate dehydrogenase kinase isozyme 4 (PDK4). GLUT4 is an important glucose transporter in cardiomyocytes, and PDK4 regulates GLUT4 and insulin resistance. The SR group showed increased levels of GLUT4 expression and decreased PDK4 expression (Fig. 7*A*). Serum triacylglycerol and nonesterified fatty acid levels were also increased in this model, and further increases were observed in the CL group (Fig. 7*B*).

β_3AR antagonist improved mitochondrial ATP synthesis in the endotoxin model. To determine whether β_3AR agonists affect mitochondrial energy metabolism, we performed Western blot analysis for proteins that are involved in mitochondrial oxidative phosphorylation (OXPHOS), which represents the main source of ATP and the main site of oxygen consumption.

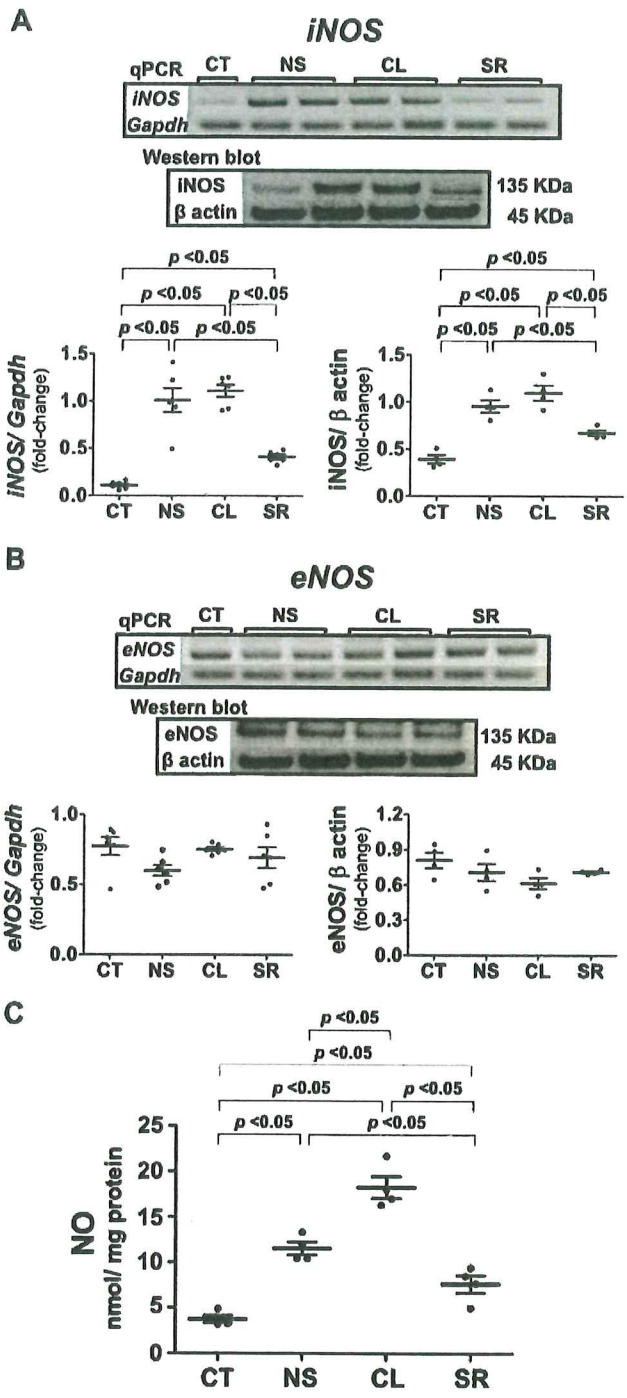

Fig. 5. Inducible nitric oxide synthase (iNOS) and endothelial nitric oxide synthase (eNOS) mRNA expression and nitric oxide (NO) concentrations in myocardium. *A*: quantitative PCR (qPCR) and Western blot analyses show significantly reduced iNOS mRNA and protein expression in the SR59230A (SR) group but significant increases in the normal saline (NS) and CL316243 (CL) groups. *B*: eNOS expression did not differ significantly between treatment groups. *C*: NO concentrations were increased in LPS-induced heart failure. CL further induced NO production, whereas SR suppressed LPS-induced NO; n = 5–7 in each group. CT, control.

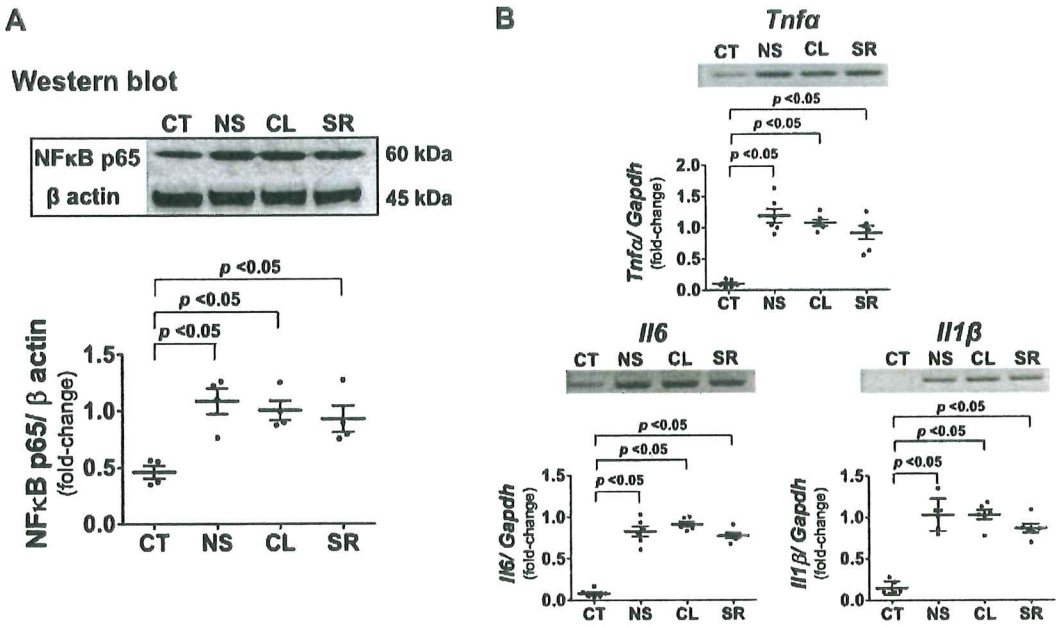

Fig. 6. Inflammatory mediators in myocardium tissues. *A*: nuclear factor kappa-B (NF-κB) plays a crucial role in inflammatory and immune responses. NF-κB protein expression was increased by LPS but did not differ significantly between normal saline (NS), CL316243 (CL), and SR59230A (SR) groups. *B*: Tnfα, Il1β, and Il6 mRNA expression levels. There were no significant differences between NS, CL, and SR groups; $n = 4-6$ in each group. CT, control.

We examined the five membrane-straddling OXPHOS complexes CI-CV in LPS-treated myocardium tissues and observed no changes in the SR or control groups but observed significant reductions in the CL group compared with the NS group (Fig. 8).

Oil red O staining. Oil red O staining revealed myocardial lipid droplets (LDs) in the NS and CL groups (Fig. 9*A*). In particular, neutral LDs were abundantly randomly scattered throughout the cytoplasm of cardiomyocytes in the CL group. In contrast, similar to the normal control group, few LDs were observed in myocardial tissues of the SR group.

Scanning electron microscope analyses. To investigate three-dimensional (3-D) subcellular ultrastructures of myocardium tissues, we macerated tissues from control and treated mice (NS, CL, and SR) using osmium and then performed SE analyses (Fig. 9*B*). Membranous cell organelles, such as mitochondria and endoplasmic reticulum, were clearly observed in these experiments because myofibrils were removed during the osmium maceration procedure. Myocardial mitochondria from control mice were round and had plate-shaped cristae that were densely packed in the matrix space. In the NS, CL, and SR treatment groups, no significant differences in 3-D ultrastructures of mitochondria were observed compared with controls. However, anomalous LDs were prominent in the CL and NS groups compared with those in the myocardial tissues of the SR and control groups. These results corresponded well with the light microscopy analyses of oil red O-stained tissues.

Immunohistochemical findings. Immunohistochemical staining of COX-1 demonstrated that mitochondrial OXPHOS was decreased in the NS and CL groups (Fig. 9*C*). In contrast, greater COX-1 expression levels were observed in tissues of the SR group than the NS group. COX-1 expression was quantified using ImageJ software, as shown in Fig. 9*D*.

DISCUSSION

To our knowledge, this study is the first to show that inhibition of β_3AR improves survival rates and ameliorates cardiac dysfunction during endotoxin-induced heart failure. No specific treatments for sepsis-related cardiac dysfunction have yet been established, and the prognosis remains extremely poor. As reported for other types of heart failure, we confirmed that β_3AR expression is enhanced under conditions of LPS-induced heart failure.

LPS is a vital structural component of gram-negative bacteria and has been identified as a pattern recognition molecule in endotoxemia. Such pathogen-associated molecular patterns can induce immune receptor activation in inflammatory and myocardial cells after binding to toll-like receptors, which are transmembrane glycoproteins that recognize pathogen-associated molecular patterns and mediate inflammatory responses through the NF-κB pathway. Accordingly, LPS injection models are widely used in studies of sepsis. Moreover, endotoxin-induced heart failure reportedly causes myocardial damage and proinflammatory injury via NF-κB.

Because TNFα and IL1β converge during the early stages of inflammation, cardiac dysfunction that is prolonged by sepsis cannot be explained by the effects of these inflammatory cytokines alone. Congruently, anticytokine therapy does not affect the prognoses for patients who have had heart failure. During the early stages of sepsis, NO, which is produced by iNOS, forms peroxynitrite and suppresses l-type Ca^{2+} channel function. In addition, NO reduces electron transport chain complex activity in myocardial mitochondria, thus contributing to mitochondrial dysfunction. Furthermore, by suppressing increases and indirect protein kinase A activities of inhibitory G proteins, β-adrenergic

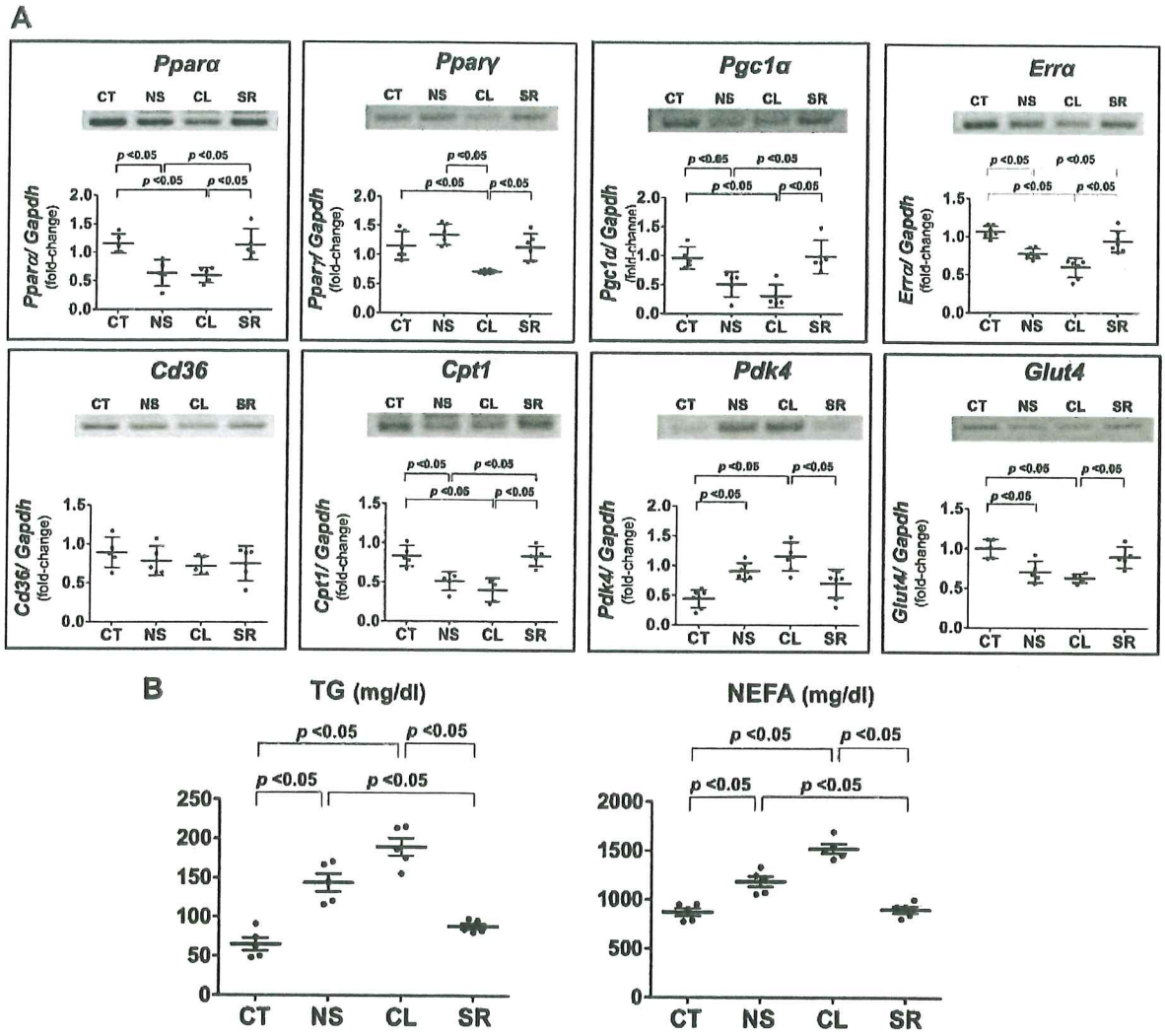

Fig. 7. Metabolic factors for ATP production in LPS-induced heart failure. *A*: quantitative PCR analyses of factors related to ATP production. Gene expression values are normalized to those of *Gapdh* mRNA. The transcription factor peroxisome proliferator-activated receptor-α (Pparα) promotes fatty acid oxidation and was significantly induced in the SR59230A (SR) group. The transcription factor peroxisome proliferator-activated receptor-γ (Pparγ) improves inflammation and insulin resistance and was present at decreased levels in the CL316243 (CL) group. The transcription factors peroxisome proliferator-activated receptor-γ coactivator 1α (Pgc1α) and Errα promote mitochondrial biogenesis and were significantly induced in the SR group. Cluster of differentiation 36 (Cd36) transports fatty acids into cells, but its expression levels were similar in all treatment groups. Carnitine palmitoyltransferase 1 (Cpt1) transports fatty acids into mitochondria and was present at significantly increased levels in the SR group. Glucose transporter type 4 (Glut4) is a major glucose transporter, and pyruvate dehydrogenase kinase isozyme 4 (Pdk4) is a negative regulator of Glut4. The SR group had increased Glut4 and low Pdk4 expression levels. Data are presented as means ± SD; n = 5–7 in each group. *B*: triglyceride (TG) and nonesterified fatty acids (NEFA) levels were increased in the normal saline (NS) group and were both further increased in the CL group. In contrast, TG and NEFA were not increased in the SR group; n = 5 in each group. CT, control.

receptor signaling reportedly inhibits catecholamine reactivity of the myocardium.

Sepsis-related cardiac dysfunction, which manifests as left ventricular dilation and decreased LVEF, is known to be reversible. In this study, we confirmed that these changes in cardiac function are reversible within 24 h.

In addition to sepsis, myocardial β_3AR expression is enhanced under conditions of heart failure. It is possible, therefore, that β_3AR expression compensates for the downregulation of β_1AR. Niu et al. (23) showed that β_3AR agonists attenuate cardiac hypertrophy in a pressure-overloaded mouse model. Hermida et al. (16) showed that β_3AR agonists protect myocardial tissues through antifibrotic mechanisms. Accordingly, treatment with β_3AR agonists could improve conditions associated with heart failure. Nevertheless, the β_3AR agonist mirabegron failed to improve cardiac dysfunction in patients with chronic heart failure (5). Herein, most β_3AR agonist-treated mice died or had further reductions in LVEF and LVESV dilation and markedly slower recovery of cardiac function. In contrast, the present β_3AR antagonist clearly improved cardiac function and prognosis.

These differences likely reflect peculiarities of the present heart failure model, in which endotoxin treatment leads to greater metabolic failures than cardiac hypertrophy and coro-

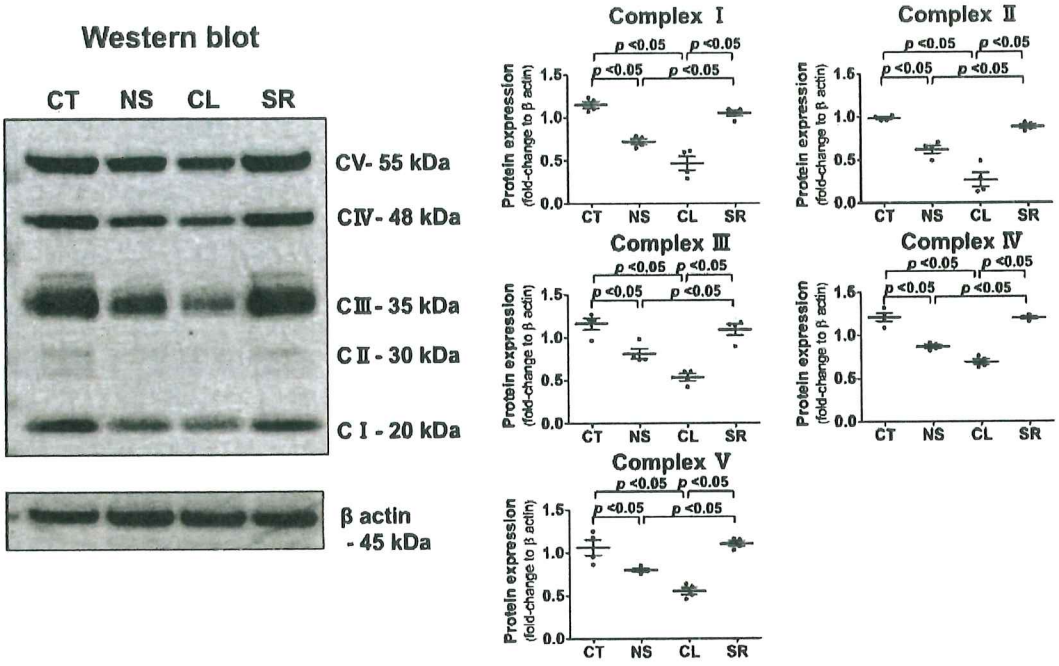

Fig. 8. Oxidative phosphorylation (OXPHOS) proteins are 5 multipeptide complexes (CI-CV) comprising over 90 different structural proteins and are encoded by nuclear and mitochondrial DNA. OXPHOS subunits together represent the mitochondrial respiratory chain that generates adenosine triphosphate (ATP). In the SR59230A (SR) group, CI-CV protein expression levels were similar to those in the control (CT) group but were significantly reduced in the CL316243 (CL) group; $n = 4$ in each group. NS, normal saline.

nary heart disease models, although myocardial damage itself may be more limited.

Yang et al. (37) reported that β_3AR levels and cardiac function changed after LPS injections. We confirmed that β_3AR was more abundantly expressed at 6–12 h than 24 h after LPS injections. In addition, β_3AR expression levels did not differ from those in the control group, in which all animals survived for 24 h or more (Supplemental Fig. S3). In the present study, cardiac function was lowest at 6 h after LPS treatments, and survival rates were lowest at 12 h. It is of note that β_3AR expression was significantly reduced at 18 h after LPS administration in the SR group compared with the NS and CL groups. This result suggests a relationship between β_3AR expression and recovery of cardiac function.

Recent studies associate inflammation-induced mitochondrial dysfunction with impaired myocardial metabolism (3, 12, 34). In particular, cardiac dysfunction and energy depletion were related primarily to impaired fatty acid oxidation and consequent reductions in ATP synthesis. Free fatty acids (FFAs) cross cells via CD36, and some react with CPT1 enzymes and enter mitochondria for fatty acid oxidation. The remaining FFAs are stored in cells as triglycerides. Under conditions of impaired fatty acid oxidation, energy production shifts to glycolysis, and in cardiac muscle cells, this requires glucose transport via GLUT4. Intracellular glucose then enters glycolysis, which is regulated by PDK4. Both glucose and FFA metabolic pathways are regulated by PPARα, PGC1α, or ERRα. In failing hearts, myocardial energy supply is known to shift from fatty acid metabolism to glucose metabolism. However, this transition may also be impaired under conditions of sepsis. In the present heart model of sepsis, fatty acid and glucose metabolism were impaired, with decreased PPARα, PGC1α, and ERRα expression levels. As a result, ATP production was significantly decreased, and the resulting ATP deficiency was exacerbated by the β_3AR agonist but not by the β_3AR antagonist.

To investigate changes in fatty acid uptake into the myocardium, we examined the expression levels of the fatty acid cell membrane transporter CD36 and the mitochondrial FFA transporter CPT1. Although several studies have reported that CD36 expression decreases with sepsis (13, 28, 35), our results showed that CD36 expression was not changed significantly at 12 h after LPS administration, but it was decreased significantly in both the NS and CL groups at 6 h (Supplemental Fig. S4). These observations may reflect the timing of increases in CD36 expression after LPS insult because previous reports show such changes in CD36 expression within 6–9 h (10, 11). CD36 expression likely recovered by 12 h. CPT1 expression also decreased in the present model. Therefore, cardiac dysfunction was prolonged by ATP depletion because of impaired fatty acid transportation. Deficits of CPT1 expression destabilize the supply-demand balance of fatty acids and trigger lipid accumulation. Poor availability of lipids in the myocardium leads to mitochondrial dysfunction and insufficient energy metabolism. Therefore, the β_3AR agonist might enhance lipid accumulation, leading to lipotoxicity, which is known to cause cardiac dysfunction (30–32). The β_3AR antagonist, in contrast, suppressed losses of CPT1 expression, maintained high ATP levels, and prevented lipid accumulation. However, lipid accumulation is not always harmful. Mizuno et al. (20) reported protective aspects of LDs that play roles in the cardioprotection afforded by empagliflozin. Several reports demonstrate lipid

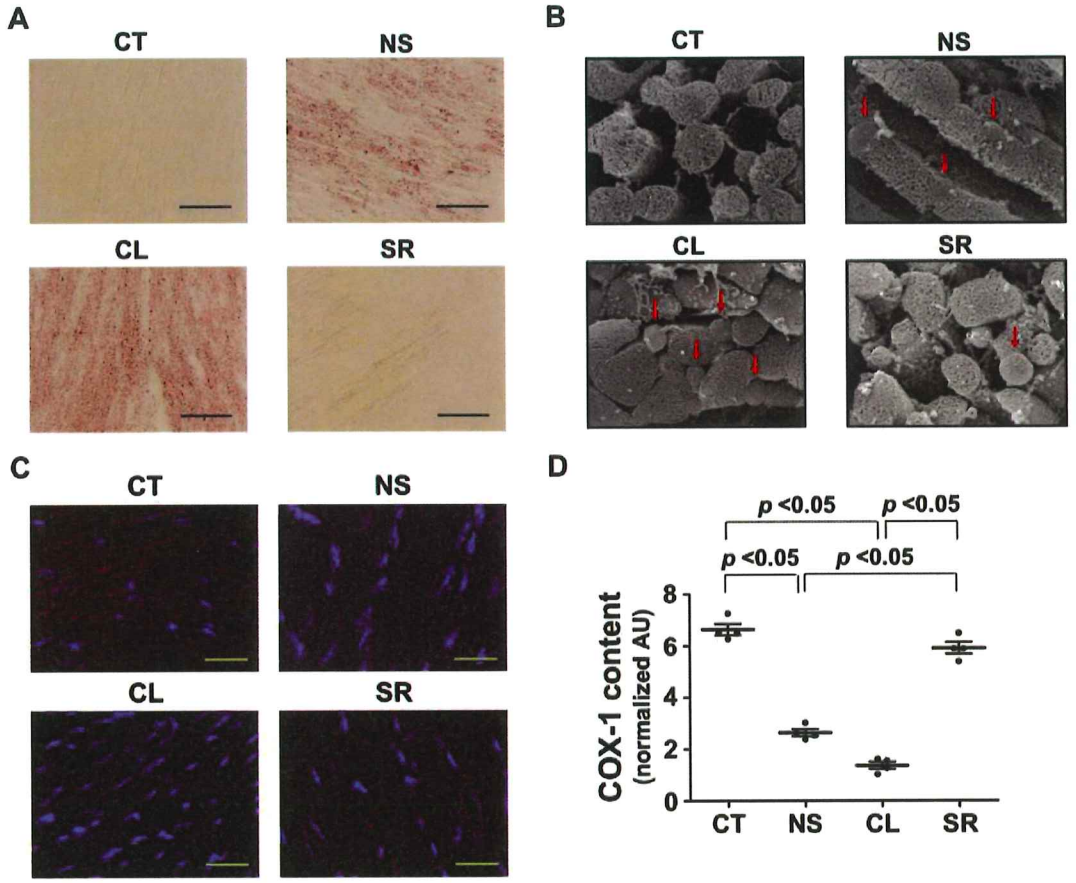

Fig. 9. Histological analyses of LPS-impaired myocardium. *A*: oil red O staining demonstrates the accumulation of lipid droplets (LDs) in heart tissues. The CL316243 (CL) group displayed abundant scattered LDs that had not been utilized for fatty acid oxidation, whereas the SR59230A (SR) group displayed few droplets, similar to the control (CT) group. *Inset*: higher magnification image of the boxed region; the bar indicates 100 μm. *B*: electron microscope analyses show LDs in LPS-induced heart tissues. The CL group showed high quantities of LDs compared with those in the SR groups. Red arrows indicate LDs. *C*: representative images of histological sections and fluorescence immunostaining for cytochrome-*c* oxidase-1 (COX-1) expression (red); nuclei were counterstained with Hoechst 33258 (blue). COX-1 expression was clearly suppressed in normal saline (NS) and CL groups. In contrast, COX-1 expression was induced in the SR group. The bar indicates 20 μm. *D*: COX-1 expression was quantified using ImageJ software; $n = 5$ in each group. AU, arbitrary units; CT, control.

accumulation in the myocardium of LPS model and show that ceramide accumulation suppresses cardiac function (6, 24). Collectively, these studies suggest that the causal relationship between β_3AR and septic heart failure is mediated by lipid metabolism. Furthermore, sepsis-related cardiac dysfunction was reversible. These results elucidate mechanisms of sepsis-related heart failure.

As shown in several studies (7, 25, 28, 33), our LPS model demonstrates reduced expression of PPARα and a tendency for increased PPARγ expression. However, our results showed that compared with the β_3AR antagonist, the β_3AR agonist significantly reduced both PPARα and PPARγ expression levels in septic hearts. Because PPAR expression levels decreased, myocardial energy production was likely suppressed, owing to impairment of glycolysis and fatty acid oxidation. These results suggest that the β_3AR agonist depletes myocardial energy and disrupts cardiac function. In contrast, the β_3AR antagonist prevented deterioration of fatty acid metabolism during the acute phase of sepsis.

At another level, NO pathway stimulation by β_3AR likely contributes to the deterioration of cardiac function during sepsis. Reportedly, iNOS is expressed in response to inflammation and produces large quantities of NO (29). Bougaki et al. (4) also reported that eNOS activity reduced the synthesis of inflammatory cytokines and prevented myocardial dysfunction in an experimental sepsis model. However, these observations suggest that NO synthesis, induced by eNOS, contributes to early myocardial dysfunction under the conditions of sepsis (15). Increased iNOS expression plays a key role in the late-onset cardiac dysfunction that is associated with sepsis. β_3AR agonists reportedly promote negative inotropic effects through NO production (17, 36), and in excess, NO is converted to the cytotoxic radical peroxynitrate (19, 21, 22). Hence, the β_3AR antagonist has therapeutic potential to reduce myocardial damage by limiting NO production and maintaining cardiac energy production during the acute phase of sepsis. In our experiments, the β_3AR antagonist significantly reduced iNOS production strongly, especially in comparison with the effects of the β_3AR agonist.

NF-κB expression was enhanced in the myocardium following stimulation with LPS, but this change was not significant, not even with regulators of β_3AR. Other inflammatory cyto-

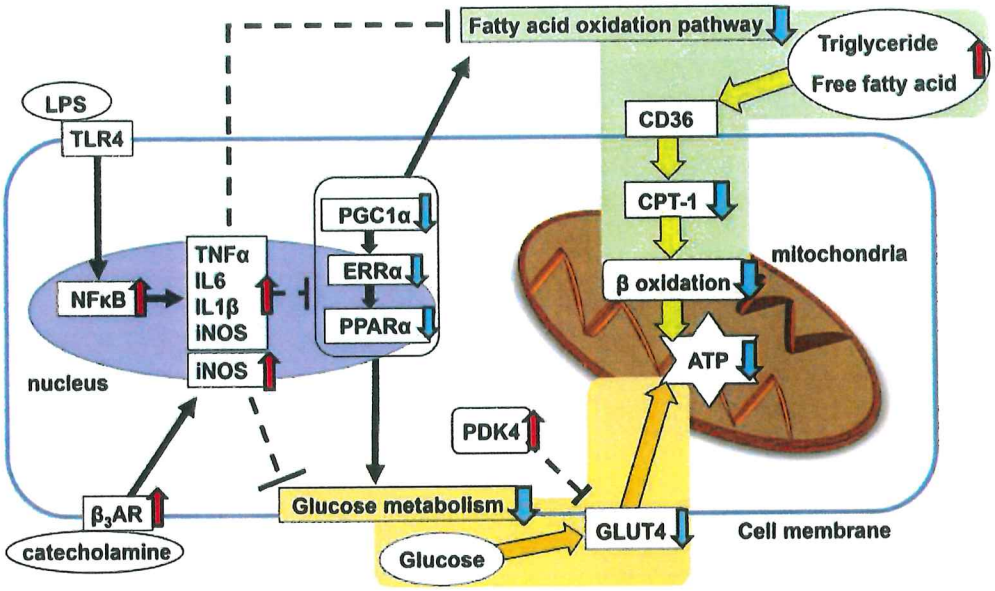

Fig. 10. Schematic diagram of the association between inflammatory mediators and metabolic pathways in LPS-induced heart failure. The LPS receptor toll-like receptor 4 (TLR4) plays a crucial role in the initiation of inflammation. LPS-activated TLR4 induces inflammatory mediators such as TNFα, IL1β, IL6, and inducible nitric oxide synthase (iNOS) by activating nuclear factor-κB (NF-κB), leading to impaired cardiac ATP production. Inflammatory mediators inhibit cardiac metabolism, such as mitochondrial transcriptional activities, fatty acid oxidation, and glucose metabolism. β_3-Adrenergic receptor (AR)-related iNOS expression enhanced these signaling pathways. Red arrows indicate upregulation of each factor. Blue arrows indicate downregulation of each factor. CD36, cluster of differentiation 36; CPT-1, carnitine palmitoyltransferase 1; ERRα, estrogen-related receptor-α; GLUT4, glucose transporter type 4; PDK4, pyruvate dehydrogenase kinase isozyme 4; PGC1α, peroxisome proliferator-activated receptor-γ coactivator 1α; PPARα, peroxisome proliferator-activated receptor-α.

kines were also unresponsive to β_3AR regulators, suggesting that NO production is independent of NF-κB and regulated via β_3AR. In vitro experiments in rat cardiomyoblasts showed that LPS-induced iNOS expression and NO production are significantly dependent on β_3AR. These experiments also revealed no changes in the expression of NF-κB, further indicating that β_3AR regulates iNOS expression independently of NF-κB. Hence, we conclude that β_3AR antagonists can prevent cardiac dysfunction by inhibiting iNOS expression under conditions of endotoxin-induced heart failure. We present a schematic diagram of LPS-induced cardiac metabolism in Fig. 10.

Mitochondrial dysfunction is considered a cause of sepsis-related cardiac dysfunction (3, 12, 34). In the present model, the β_3AR antagonist increased PGC1α, ERRα, and PPARα expression, further suggesting favorable effects on mitochondrial biogenesis and ATP synthesis. In agreement, our immunohistochemical analyses showed enhanced expression of COX-1 in the presence of the β_3AR antagonist. This enzyme is key to aerobic metabolism in the mitochondrial intermembrane. In this study, we demonstrate the possibility that suppression of β_3AR could improve mitochondrial function in endotoxin-induced heart failure; however, as the evidence was indirect, further research is required.

The present histological images from the LPS-treated model corroborate our hypotheses. Specifically, LDs were observed in the myocardium, with substantial numbers in the CL group. Decreased COX-1 expression also suggested mitochondrial dysfunction in the CL group. In electron microscope images, abnormal accumulations of LDs can be observed around the mitochondria, most prominently in myocardium tissues of the NS and CL groups. However, no apparent abnormalities in 3-D ultrastructures of mitochondria were observed. These findings suggest that endotoxin-induced heart failure was caused by a disorder of fatty acid transport.

Herein, we demonstrate that inhibition of the β_3AR suppresses endotoxin-induced heart failure and improves prognoses by restoring mitochondrial biogenesis and regulating cardiac metabolism. These data suggest roles of the β_3AR in septic heart failure, especially during the acute catabolic phase, and indicate differing mechanisms from those of other types of heart failure, such as coronary heart disease.

Conclusion

The results of this study suggested that endotoxin-induced heart failure is influenced by fatty acid and glucose metabolism. Blockade of the β_3AR ameliorated cardiac function and mortality by maintaining cardiac energy metabolism and mitochondrial biogenesis. The β_3AR may be a metabolic target for the treatment of sepsis-related heart failure. Further studies are required to examine the effectiveness of β_3AR antagonists as treatments from other types of heart failure.

GRANTS

The present study was supported by Japan Society for the Promotion of Science Grant JP15K10965.

DISCLOSURES

No conflicts of interest, financial or otherwise, are declared by the authors.

AUTHOR CONTRIBUTIONS

M.O. conceived and designed research; S.K., M.O., E.I., D.K., K.H., and Y.K. performed experiments; S.K., M.O., E.I., D.K., T.W., K.H., S.F., and

N.H. analyzed data; S.K., M.O., T.W., S.F., and N.H. interpreted results of experiments; S.K. prepared figures; M.O. drafted manuscript; M.O. edited and revised manuscript; M.O. approved final version of this manuscript.

REFERENCES

1. **Annane D, Bellissant E, Cavaillon JM.** Septic shock. *Lancet* 365: 63–78, 2005. doi:10.1016/S0140-6736(04)17667-8.
2. **Aragón JP, Condit ME, Bhushan S, Predmore BL, Patel SS, Grinsfelder DB, Gundewar S, Jha S, Calvert JW, Barouch LA, Lavu M, Wright HM, Lefer DJ.** Beta3-adrenoreceptor stimulation ameliorates myocardial ischemia-reperfusion injury via endothelial nitric oxide synthase and neuronal nitric oxide synthase activation. *J Am Coll Cardiol* 58: 2683–2691, 2011. doi:10.1016/j.jacc.2011.09.033.
3. **Arulkumaran N, Deutschman CS, Pinsky MR, Zuckerbraun B, Schumacker PT, Gomez H, Gomez A, Murray P, Kellum JA; ADQI XIV Workgroup.** Mitochondrial function in sepsis. *Shock* 45: 271–281, 2016. doi:10.1097/SHK.0000000000000463.
4. **Bougaki M, Searles RJ, Kida K, Yu J, Buys ES, Ichinose F.** Nos3 protects against systemic inflammation and myocardial dysfunction in murine polymicrobial sepsis. *Shock* 34: 281–290, 2010. doi:10.1097/SHK.0b013e3181cdc327.
5. **Bundgaard H, Axelsson A, Hartvig Thomsen J, Sørgaard M, Kofoed KF, Hasselbalch R, Fry NA, Valeur N, Boesgaard S, Gustafsson F, Køber L, Iversen K, Rasmussen HH.** The first-in-man randomized trial of a beta3 adrenoceptor agonist in chronic heart failure: the BEAT-HF trial. *Eur J Heart Fail* 19: 566–575, 2017. doi:10.1002/ejhf.714.
6. **Chung HY, Kollmey AS, Schrepper A, Kohl M, Bläss MF, Stehr SN, Lupp A, Gräler MH, Claus RA.** Adjustment of dysregulated ceramide metabolism in a murine model of sepsis-induced cardiac dysfunction. *Int J Mol Sci* 18: E839, 2017. doi:10.3390/ijms18040839.
7. **Crossland H, Constantin-Teodosiu D, Gardiner SM, Greenhaff PL.** Peroxisome proliferator-activated receptor γ agonism attenuates endotoxaemia-induced muscle protein loss and lactate accumulation in rats. *Clin Sci (Lond)* 131: 1437–1447, 2017. doi:10.1042/CS20170958.
8. **Dal-Secco D, DalBó S, Lautherbach NES, Gava FN, Celes MRN, Benedet PO, Souza AH, Akinaga J, Lima V, Silva KP, Kiguti LRA, Rossi MA, Kettelhut IC, Pupo AS, Cunha FQ, Assreuy J.** Cardiac hyporesponsiveness in severe sepsis is associated with nitric oxide-dependent activation of G protein receptor kinase. *Am J Physiol Heart Circ Physiol* 313: H149–H163, 2017. doi:10.1152/ajpheart.00052.2016.
9. **de Montmollin E, Aboab J, Mansart A, Annane D.** Bench-to-bedside review: β-adrenergic modulation in sepsis. *Crit Care* 13: 230, 2009. doi:10.1186/cc8026.
10. **Drosatos K, Drosatos-Tampakaki Z, Khan R, Homma S, Schulze PC, Zannis VI, Goldberg IJ.** Inhibition of c-Jun-N-terminal kinase increases cardiac peroxisome proliferator-activated receptor α expression and fatty acid oxidation and prevents lipopolysaccharide-induced heart dysfunction. *J Biol Chem* 286: 36331–36339, 2011. doi:10.1074/jbc.M111.272146.
11. **Drosatos K, Khan RS, Trent CM, Jiang H, Son NH, Blaner WS, Homma S, Schulze PC, Goldberg IJ.** Peroxisome proliferator-activated receptor-γ activation prevents sepsis-related cardiac dysfunction and mortality in mice. *Circ Heart Fail* 6: 550–562, 2013. doi:10.1161/CIRCHEARTFAILURE.112.000177.
12. **Durand A, Duburcq T, Dekeyser T, Neviere R, Howsam M, Favory R, Preau S.** Involvement of mitochondrial disorders in septic cardiomyopathy. *Oxid Med Cell Longev* 2017: 1–13, 2017. doi:10.1155/2017/4076348.
13. **Feingold KR, Moser A, Patzek SM, Shigenaga JK, Grunfeld C.** Infection decreases fatty acid oxidation and nuclear hormone receptors in the diaphragm. *J Lipid Res* 50: 2055–2063, 2009. doi:10.1194/jlr.M800655-JLR200.
14. **Figueroa XF, Poblete I, Fernández R, Pedemonte C, Cortés V, Huidobro-Toro JP.** NO production and eNOS phosphorylation induced by epinephrine through the activation of beta-adrenoceptors. *Am J Physiol Heart Circ Physiol* 297: H134–H143, 2009. doi:10.1152/ajpheart.00023.2009.
15. **Gorressen S, Stern M, van de Sandt AM, Cortese-Krott MM, Ohlig J, Rassaf T, Gödecke A, Fischer JW, Heusch G, Merx MW, Kelm M.** Circulating NOS3 modulates left ventricular remodeling following reperfused myocardial infarction. *PLoS One* 10: e0120961, 2015. doi:10.1371/journal.pone.0120961.
16. **Hermida N, Michel L, Esfahani H, Dubois-Deruy E, Hammond J, Bouzin C, Markl A, Colin H, Steenbergen AV, De Meester C, Beauloye C, Horman S, Yin X, Mayr M, Balligand JL.** Cardiac myocyte β3-adrenergic receptors prevent myocardial fibrosis by modulating oxidant stress-dependent paracrine signaling. *Eur Heart J* 39: 888–898, 2018. doi:10.1093/eurheartj/ehx366.
17. **Khadour FH, Panas D, Ferdinandy P, Schulze C, Csont T, Lalu MM, Wildhirt SM, Schulz R.** Enhanced NO and superoxide generation in dysfunctional hearts from endotoxemic rats. *Am J Physiol Heart Circ Physiol* 283: H1108–H1115, 2002. doi:10.1152/ajpheart.00549.2001.
18. **Kleindienst A, Battault S, Belaidi E, Tanguy S, Rosselin M, Boulghobra D, Meyer G, Gayrard S, Walther G, Geny B, Durand G, Cazorla O, Reboul C.** Exercise does not activate the β3 adrenergic receptor-eNOS pathway, but reduces inducible NOS expression to protect the heart of obese diabetic mice. *Basic Res Cardiol* 111: 40, 2016. doi:10.1007/s00395-016-0559-0.
19. **Lancel S, Tissier S, Mordon S, Marechal X, Depontieu F, Scherpereel A, Chopin C, Neviere R.** Peroxynitrite decomposition catalysts prevent myocardial dysfunction and inflammation in endotoxemic rats. *J Am Coll Cardiol* 43: 2348–2358, 2004. doi:10.1016/j.jacc.2004.01.047.
20. **Mizuno M, Kuno A, Yano T, Miki T, Oshima H, Sato T, Nakata K, Kimura Y, Tanno M, Miura T.** Empagliflozin normalizes the size and number of mitochondria and prevents reduction in mitochondrial size after myocardial infarction in diabetic hearts. *Physiol Rep* 6: e13741, 2018. doi:10.14814/phy2.13741.
21. **Moniotte S, Kobzik L, Feron O, Trochu JN, Gauthier C, Balligand JL.** Upregulation of $\beta_{(3)}$-adrenoceptors and altered contractile response to inotropic amines in human failing myocardium. *Circulation* 103: 1649–1655, 2001. doi:10.1161/01.CIR.103.12.1649.
22. **Mungrue IN, Gros R, You X, Pirani A, Azad A, Csont T, Schulz R, Butany J, Stewart DJ, Husain M.** Cardiomyocyte overexpression of iNOS in mice results in peroxynitrite generation, heart block, and sudden death. *J Clin Invest* 109: 735–743, 2002. doi:10.1172/JCI0213265.
23. **Niu X, Watts VL, Cingolani OH, Sivakumaran V, Leyton-Mange JS, Ellis CL, Miller KL, Vandegaer K, Bedja D, Gabrielson KL, Paolocci N, Kass DA, Barouch LA.** Cardioprotective effect of beta-3 adrenergic receptor agonism: role of neuronal nitric oxide synthase. *J Am Coll Cardiol* 59: 1979–1987, 2012. doi:10.1016/j.jacc.2011.12.046.
24. **Park TS, Hu Y, Noh HL, Drosatos K, Okajima K, Buchanan J, Tuinei J, Homma S, Jiang XC, Abel ED, Goldberg IJ.** Ceramide is a cardiotoxin in lipotoxic cardiomyopathy. *J Lipid Res* 49: 2101–2112, 2008. doi:10.1194/jlr.M800147-JLR200.
25. **Peng S, Xu J, Ruan W, Li S, Xiao F.** PPAR-γ activation prevents septic cardiac dysfunction via inhibition of apoptosis and necroptosis. *Oxid Med Cell Longev* 2017: 1–11, 2017. doi:10.1155/2017/8326749.
26. **Rudiger A, Singer M.** Mechanisms of sepsis-induced cardiac dysfunction. *Crit Care Med* 35: 1599–1608, 2007. doi:10.1097/01.CCM.0000266683.64081.02.
27. **Sakai M, Suzuki T, Tomita K, Yamashita S, Palikhe S, Hattori K, Yoshimura N, Matsuda N, Hattori Y.** Diminished responsiveness to dobutamine as an inotrope in mice with cecal ligation and puncture-induced sepsis: attribution to phosphodiesterase 4 upregulation. *Am J Physiol Heart Circ Physiol* 312: H1224–H1237, 2017. doi:10.1152/ajpheart.00828.2016.
28. **Schilling J, Lai L, Sambandam N, Dey CE, Leone TC, Kelly DP.** Toll-like receptor-mediated inflammatory signaling reprograms cardiac energy metabolism by repressing peroxisome proliferator-activated receptor γ coactivator-1 signaling. *Circ Heart Fail* 4: 474–482, 2011. doi:10.1161/CIRCHEARTFAILURE.110.959833.
29. **Schulz R, Rassaf T, Massion PB, Kelm M, Balligand JL.** Recent advances in the understanding of the role of nitric oxide in cardiovascular homeostasis. *Pharmacol Ther* 108: 225–256, 2005. doi:10.1016/j.pharmthera.2005.04.005.
30. **Schulze PC, Drosatos K, Goldberg IJ.** Lipid use and misuse by the heart. *Circ Res* 118: 1736–1751, 2016. doi:10.1161/CIRCRESAHA.116.306842.
31. **Sharma S, Adrogue JV, Golfman L, Uray I, Lemm J, Youker K, Noon GP, Frazier OH, Taegtmeyer H.** Intramyocardial lipid accumulation in the failing human heart resembles the lipotoxic rat heart. *FASEB J* 18: 1692–1700, 2004. doi:10.1096/fj.04-2263com.
32. **Simon JN, Chowdhury SA, Warren CM, Sadayappan S, Wieczorek DF, Solaro RJ, Wolska BM.** Ceramide-mediated depression in cardiomyocyte contractility through PKC activation and modulation of myofilament protein phosphorylation. *Basic Res Cardiol* 109: 445, 2014. doi:10.1007/s00395-014-0445-6.
33. **Standage SW, Bennion BG, Knowles TO, Ledee DR, Portman MA, McGuire JK, Liles WC, Olson AK.** PPARα augments heart function and cardiac fatty acid oxidation in early experimental polymicrobial sepsis. *Am*

J Physiol Heart Circ Physiol 312: H239–H249, 2017. doi:10.1152/ajpheart.00457.2016.

34. **Suzuki T, Suzuki Y, Okuda J, Kurazumi T, Suhara T, Ueda T, Nagata H, Morisaki H.** Sepsis-induced cardiac dysfunction and β-adrenergic blockade therapy for sepsis. *J Intensive Care* 5: 22, 2017. doi:10.1186/s40560-017-0215-2.
35. **Tessier JP, Thurner B, Jüngling E, Lückhoff A, Fischer Y.** Impairment of glucose metabolism in hearts from rats treated with endotoxin. *Cardiovasc Res* 60: 119–130, 2003. doi:10.1016/S0008-6363(03)00320-1.
36. **van de Sandt AM, Windler R, Gödecke A, Ohlig J, Zander S, Reinartz M, Graf J, van Faassen EE, Rassaf T, Schrader J, Kelm M, Merx MW.** Endothelial NOS (NOS3) impairs myocardial function in developing sepsis. *Basic Res Cardiol* 108: 330, 2013. doi:10.1007/s00395-013-0330-8.
37. **Yang N, Shi XL, Zhang BL, Rong J, Zhang TN, Xu W, Liu CF.** The trend of β3-adrenergic receptor in the development of septic myocardial depression: a lipopolysaccharide-induced rat septic shock model. *Cardiology* 139: 234–244, 2018. doi:10.1159/000487126.